Nat. Hazards Earth Syst. Sci. Discuss., doi:10.5194/nhess-2016-191, 2016
Manuscript under review for journal Nat. Hazards Earth Syst. Sci.
Published: 4 July 2016

Natural Hazards and Earth System Sciences
Open Access
Discussions

Identification of high risk zones for geological origin hazards using PALSAR-2 remote sensing data: Kelantan river basin, Peninsular Malaysia

Amin Beiranvand Pour *, Mazlan Hashim

Geoscience and Digital Earth Centre (Geo-DEC)

Research Institute for Sustainability and Environment (RISE)

Universiti Teknologi Malaysia, 81310 UTM JB, Malaysia

Abstract

Identification of high potential risk and susceptible zones for natural hazards of geological origin is one of the most important applications of advanced remote sensing technology. In this study, the recently launched Phased Array type L-band Synthetic Aperture Radar-2 (PALSAR-2) onboard the Advanced Land Observing Satellite-2 (ALOS-2), remote sensing data were used to map geologic structural and topographical features in the Kelantan river basin for identification of high potential risk and susceptible zones for landslides and flooding areas. The data were processed for comprehensive analysis of major geological structures and detailed characterizations of lineaments, drainage patterns and lithology at both regional and district scales. Red-Green-Blue (RGB) colour-composite was applied to different polarization channels of PALSAR-2 data to extract variety of geological information. Directional convolution filters were applied to the data for identifying linear features in particular directions and edge enhancement in the spatial domain. Results indicate that lineament occurrence at regional scale was mainly linked to the N-S trending of the Bentong-Raub Suture Zone (BRSZ) in the west and Lebir Fault Zone in the east of the Kelantan state. Combination of different polarization channels produced image maps contain important information related to water bodies, wetlands and lithological units. The N-S, NE-SW and NNE-SSW lineament trends and dendritic, sub-dendritic and rectangular drainage patterns were detected in the Kelantan river basin. The analysis of field investigations data indicate that many of flooded areas were associated with high potential risk zones for hydro-geological hazards such as wetlands, urban areas, floodplain scroll, meander bend, dendritic and sub-dendritic drainage patterns, which are located in flat topography regions. Numerous landslide points were located in rectangular drainage system that associated with topographic slope of metamorphic and quaternary rock units. Consequently, structural and topographical geology maps were produced for Kelantan river basin using PALSAR-2 data, which could be broadly applicable for landslide hazard mapping and identification of high potential risk zone for hydro-geological hazards. Geo-hazard mitigation programmes could be conducted in the landslide recurrence regions and flooded areas for reducing natural catastrophes leading to loss of financial investments and death in the Kelantan river basin. In this investigation, PALSAR-2 has proven to be successful advanced earth observation satellite data for disasters monitoring in tropical environments.

Key words: ALOS-2; PALSAR-2; Geological origin hazards; Tropical environments; Peninsular Malaysia

*Corresponding Author. Tel: +607 -5530666; Fax: +607- 5531174; Email address: beiranvand.amin80@gmail.com; a.beiranvand@utm.my; mazlanhashim@utm.my

1. Introduction

Advances in remote sensing technology allow the application of Synthetic Aperture Radar (SAR) data in geological structural analysis for tropical environments (Shimada and Isoguchi, 2002; Morelli and Piana, 2006; Ramli et al., 2009; Pour and Hashim, 2013, 2014a,b, 2015a,b). Structural field mapping is often difficult in heavily vegetated Terrain. This is the case with the study area where dense vegetation cover, deep weathering and scarcity of bedrock exposure hampers geological structure mapping over a long distance. In addition, the use of optical remote sensing data is limited due to the persistent cloud coverage of the study area for most part of the year (Ramli et al., 2009; Hashim et al., 2013). SAR data contain potential to penetrate cloud and vegetation and unlike the optical data are dependent upon the surface roughness of the materials, ideally suited to mapping lineaments (faults and fractures) in tropical environments. Lineaments are related to large structural fractures, which represent zones of weakness in the brittle part of the lithosphere. The presence of linear tectonic structures is one of the important factors in geological hazard occurrences (Bannert, 2000a,b). Lineaments are represented by faults (linear features), lithological contacts between rock units and drainage patterns in any area (van der Pluijm and Marshak, 1997). Observation from satellite images (Landsat Thematic Mapper) in the Himalayan Mountains of Nepal and China revealed a clear connection between of active faults, associated with earthquakes and the occurrence of large landslides (Bannert, 2000a,b). Therefore, delineation of faults and fractures using advanced remote sensing technology in any region is necessity to assess the potential for many natural geological hazards. Numerous investigations have used faults, drainage patterns and lithology factors as important factors to measure and map the susceptibility of geological hazard (Guzzetti et al., 1999; Dai and Lee, 2002; Suzen and Doyuran, 2004; Abdullah et al., 2013).

The Advanced Land Observing Satellite-2 (ALOS-2) was launched on May 24, 2014 as successor of ALOS-1 (launched on January 24, 2006 and decommissioned in May 2011) (http://global.jaxa.jp/press/2014/05/20140524_daichi2.html; Blau, 2014). The ALOS-2 is exclusively installed with the Phased Array type L-band Synthetic Aperture Radar-2 (PALSAR-2) using microwaves to maximized its ability compare to the ALOS-1, on which three sensors (two optical and one microwave devices) were onboard (Igarashi, 2001; Suzuki et al., 2012). In particular, L-band microwave from PALSAR-2 has ability to penetrate vegetation due to relatively long wavelengths (about 24 cm), making the data particularly useful for geological structural mapping in tropical environments (Igarashi, 2001; Rosenqvist et al., 2004; ERSDAC, 2006; Arikawa et al., 2010; Yamamoto et al., 2013; Pour and Hashim, 2013, 2014 a,b, 2015a,b; Shimada et al., 2015). The wavelength of the L-band is relatively long among microwaves (C-band: about 6 cm and X- band: about 3 cm), allowing it to travel all the way down to the ground through vegetation (Woodhouse, 2006). Not only can information be, obtained about vegetation but information of the ground surface can be obtained as well. Additionally, L-band is less affected by the growth of vegetation, which is useful for SAR interference analysis (Interferometry). Therefore, L-band is capable to acquire changes on the land more precisely compared to shorter wavelength SAR when some diastrophism takes place due to an earthquake or a volcanic activity and floods or landslides caused by a natural disaster (Suzuki, 2014). Accordingly, a further increase in amount of information for geological structural mapping could be derived from the recently launched PALSAR-2 data. Analysis of the data can provide completely new insights into heavily vegetated areas threatened by natural hazards of geological origin. Consequently, the advanced SAR remote sensing data are broadly applicable for geo-environmental research to identify the causes of natural disasters and point the way to rehabilitation measures especially in tropical environments. To date, few studies used L-band SAR remote sensing data for geological structure mapping in tropical environments (Pour and Hashim, 2013, 2014a,b, 2015a,b). This study is the first time that L-band SAR remote sensing data is used for identification of high potential risk and susceptible zones for natural hazards of geological origin in tropical environments. It is dire need to apply this approach in Malaysia and other parts of South East Asia that have inaccessible regions and high potential zones for natural hazards of geological origin hidden by dense rainforest.

Yearly, several landslides occur during heavy monsoon rainfall in Kelantan river basin, Peninsular Malaysia, which are obviously connected to geological structures and topographical features of the region. In recent years especially, there have been many severe flooding events (in the year 2005, 2006, 2007, 2008, 2009, 2014 and 2015) which have led to significant damage to livestock, agricultural produce, homes and businesses in the Kelantan

Nat. Hazards Earth Syst. Sci. Discuss., doi:10.5194/nhess-2016-191, 2016
Manuscript under review for journal Nat. Hazards Earth Syst. Sci.
Published: 4 July 2016

river basin (Pradhan, 2009; Pradhan et al., 2009; Pradhan and Youssef, 2011; Tehrany et al., 2013; Nazaruddin, et al., 2014). The problem stems from the inappropriate use of lands that are vulnerable to erosion, quick water runoff and slope failure. Recent challenge is to identify high potential risk and susceptible zones for natural hazards of geological origin in the Kelantan river basin using advanced remote sensing technology. Additionally, accurate and up-dated geological structure and topographical maps are largely lacking for the Kelantan river basin. Therefore, the objectives of this study are (i) to identify high potential risk and susceptible zones for geological origin hazards using the recently launched ALOS-2-Phased Array type L-band Synthetic Aperture Radar-2 (PALSAR-2) remote sensing data in the Kelantan river basin at regional and district scales; (ii) to produce accurate geological structure and topographical maps for the Kelantan river basin using PALSAR-2 data; and (iii) to compare the detected high potential risk and susceptible zones with high damaged areas in recent flooding events in the Kelantan river basin.

2. Study area

Peninsular Malaysia is composed of central segment of Southeast Asian continental core of Sundaland (Metcalfe, 2013a,b). The state of Kelantan is located in north-eastern corner of Peninsular Malaysia (Fig. 1). Kelantan river is the major river in the region. It appears at the convergence of the Galas river and Lebir river near Kuala Kari and meanders over the coastal plain until it finally degrades into the South China Sea. Kelantan river basin covers 923 km^2, which is about 85% of the Kelantan state's surface area. It is composed of flat slope to moderately sloping areas in northern part and steep scraps and high slopes in the southern part of the river basin (Pradhan et al., 2009). A wide variety of rocks consisting of igneous, sedimentary and metamorphic rocks are distributed in a north-south trend in the Kelantan

Nat. Hazards Earth Syst. Sci. Discuss., doi:10.5194/nhess-2016-191, 2016
Manuscript under review for journal Nat. Hazards Earth Syst. Sci.
Published: 4 July 2016

state. Typically, four types of rocks are classified in the region, including granitic rocks, sedimentary/metasedimentary rocks, extrusive rocks (volcanic rocks) and unconsolidated sediments (Fig. 2). Localised geological features comprise faulting and jointing in the granitic rocks and folding, faulting and jointing in the sedimentary rocks. Granitic rocks are distributed in the west (the Main Range granite) and east borders (the Boundary Range granite) of the state of Kelantan (Rahman and Mohamed, 2001; Department of Minerals and Geoscience Malaysia, 2003; Heng et al., 2006).

The Main Range granite is located in the west of the state, which is stretched along western Kelantan up to the boundary of Perak and Pahang states and Thailand boundary (Fig. 2). The dominant structural trend in Kelantan is along N-S to NW-SE direction that derived from postorogenic phase (Ghani, 2009). The Main Range granite is located along the western margin of the Bentong-Raub Suture Zone (BRSZ) and extends north to Thailand (Schwartz et al., 1995; Metcalfe, 2000). The north-south trending Bentong-Raub Suture (approximately 13 km wide) extends from Thailand through Raub and Bentong to the east of Malacca, Peninsular Malaysia. The BRSZ is characterized by a series of parallel topographic north-south trending lineaments and the presence of small bodies of mafic to ultramafic rocks that are commonly serpentinized (Tan, 1996). The Lebir Fault Zone is located in the eastern part of Kelantan state (Fig. 2), which is one of the major lineaments in Peninsular Malaysia and considered to be post-Cretaceous and sinistral strike-slip fault (Tjia, 1989; Harun, 2002).

The landscape in the state of Kelantan has been divided into four types, including mountainous areas, hilly areas, plain areas and coastal areas (Unjah et al., 2001; Raj, 2009). Mount Chama (Gunung) is the highest point (2171m) in the Kelantan state, which is located in Gua Musang district in the western part of the state, near the border of Perak State (Nazaruddin, et al., 2014). Quaternary deposits consist of alluvium deposits or unconsolidated sediments. Triassic marine siliciclastics, volcaniclastics, sandstone and limestone are the other sedimentary rocks occur in the Kelantan state.

3. Materials

PALSAR-2 of the ALOS-2 has been significantly improved from the ALOS-1's PALSAR in all aspects, including resolution, observation band and time lag for data provision (Arikawa et al., 2010; Kankaku et al., 2010; Suzuki et al., 2012). ALOS-2 science proficiencies contain global environmental monitoring using the time-series PALSAR-2. The research objective encompasses biospheric, cryospheric, coastal ocean research and disaster monitoring and mitigation (Shimada, 2013). PALSAR-2 is a microwave sensor that emits L-band radio waves and receives their reflection from the ground to acquire information (Suzuki et al., 2012). It has three observation modes, including (i) Spotlight mode: the most detailed observation mode with 1 by 3 meters resolution and observation width of 25 km; (ii) Strip map mode: a high-resolution mode with the choice of 3 (ultra fine), 6 (high sensitivity) or 10 (fine) meters resolution and observation width of 50 or 70 km; and (iii) ScanSAR mode: a broad area observation width of 350 (nominal) or 490 (wide) km and resolution of 100 or 60 meters (Yamamoto et al., 2013; Shimada et al., 2015).

Selection of the most suitable observation mode and time acquisition of PALSAR-2 data for the research objectives will maximize the efficiency of geo-environmental monitoring works. In this investigation, a ScanSAR mode dual polarization (level 3.1) and two Fine mode dual polarization (level 3.1) PALSAR-2 scenes were obtained from ALOS-2 data distribution consortium online system Remote Sensing Technology Center of Japan (RESTEC) (http://www.restec.or.jp/english/index.html) and PASCO Corporation (http://en.alos-pasco.com; https://satpf.jp/) for comprehensive analysis of major geological structures and detailed characterizations of lineaments in the state of Kelantan. The data used in this study were acquired during dry season (June to August, 2015). Two distinct wet seasons from September to December and February to May are reported by Malaysian Meteorological Department (MMD) in Peninsular Malaysia (Mardiana et al., 2000). Precipitation and soil moisture variations have influence on detailed geologic lineament analysis using microwave signal. SAR data are highly sensitive to water content in the soil because of large contrast between dielectric properties of water and dry soil (Eagleman and Lin, 1976; Jackson and Schmugge, 1989; Lacava et al., 2005). Hence, SAR data acquired during dry seasons contain more useful information for detailed geological structural mapping in tropical environments. In this study, the ScanSAR observation mode has 60 m resolution and 490 km swath width (wide mode), and the fine observation mode contains data with 10 m resolution and 70 km swath width. Dual polarization for the both data includes HH+HV polarization images (HH= Horizontally transmitted and Horizontally received, HV= Horizontally transmitted and Vertically received). HV channel is a channel that transmits a vibrating wave in a horizontal direction against the ground (H) and receives it vertically (V). It is expected to acquire more detailed observation data on ground. Particularly, HV channel (cross-polarization) in the ScanSAR and fine observation modes increase the amount of information extraction for geological structural mapping at both regional and districts scales (Pour and Hashim, 2015a,b). HV polarization is more suitable for lineament extraction and edge enhancement in tropical environments than other polarization channels, because cross-polarization is more sensitive to lineament and also enhances penetration (Henderson and Lewis 1998; Pour and Hashim, 2015a,b). Penetration is proportional to wave-length, and cross-polarization also enhances penetration (Henderson and Lewis 1998). Therefore, HV polarization channel records more geological features that cover by dense vegetation. In the Level 3.1 product of

Nat. Hazards Earth Syst. Sci. Discuss., doi:10.5194/nhess-2016-191, 2016
Manuscript under review for journal Nat. Hazards Earth Syst. Sci.
Published: 4 July 2016

PALSAR-2, image quality corrections (noise reduction and dynamic range compression) are performed to level 1.5 of PALSAR-2 data. It should be noted that level 1.5 of PALSAR-2 data contain the following characteristics (i) range and multi-look azimuth compressed data is represented by amplitude data; (ii) range coordinate is converted from slant range to ground range; and (iii) map projection is also performed (Japan Aerospace Exploration Agency, 2014). The positioning accuracy of PALSAR-2 data is excellent and it does not always require the field survey to modify the positioning accuracy. So, it can reduce the map production time and contribute to cost reduction as well (Shimada et al., 2015). Subsequently, the data used in this study are geo-referenced. The data were processed using the ENVI (Environment for Visualizing Images) version 5.2 software package.

4. Methods

Lineaments in remote sensing images have topographic relief and are often a surface expression of 3D geological structures in the subsurface. Lineaments, associated with brittle and ductile deformation zones appear as rectilinear and curvilinear patterns in remotely sensed images. Detailed extraction of lineaments helps in reconstructing the tectonic history of a region (Clark and Wilson, 1994). Geological lineament features are attributed to paleo-tectonic and /or neo-tectonic activity of a region. The use of remote sensing data in delineation tectonically significant lineaments has been demonstrated in many geological settings (Raharimahefa and Kusky, 2007, 2009; Amri et al., 2011; Hashim et al., 2013; Hamimi et al., 2014; Pour and Hashim, 2014a,b, 2015a,b).

Spatial transforms provide reliable and robust image processing techniques to extract the spatial information from remote sensing data. The techniques help to maximize clarity, sharpness and details of features of interest towards information extraction and further analysis. Spatial convolution filtering is based primarily on the use of convolution masks. This flexibility makes convolution one of the most useful tools in image processing. The procedure could be used to enhance low and high frequency details, as well as edges in the imagery (Haralick et al., 1987; Jensen, 2005; Schowengerdt, 2007). Linear features are formed by edges in remotely sensed images. Some linear features occur as narrow lines against a background of contrasting brightness; others are the linear contact between adjacent areas of different brightness. Edge enhancement delineates these edges and makes the shapes and details comprising the image more conspicuous and easier to analyze (Jensen, 2005). It can be used in geological applications to highlight rectilinear and curvilinear patterns in remote sensing images.

Systematic image processing techniques were implemented to the PALSAR-2 data for geological structures and lineament mapping at both regional and district scales in the state of Kelantan. It is necessary to treat the speckle in radar images by filtering before it can be used in various applications (Sheng and Xia, 1996). The presence of speckle in radar images reduce the detectability of ground targets, obscures the spatial patterns of surface features and decreases the accuracy of automated image classification (Lee and Jurkevich, 1994; Sveinsson and Benediktsson, 1996). However, image quality corrections (noise reduction) have been already applied to Level 3.1 product of PALSAR-2, but some speckles (salt and pepper noise) could be still seen in the images. In this study, the median spatial convolution filter was used for noise removal and smoothing the PALSAR-2 images. The median filter is a particularly useful statistical filter in the spatial domain, which effectively remove speckle (salt and pepper noise) in radar images without eliminating fine details (Russ, 2002; Research Systems, Inc., 2008). The median operation has the effect of excluding pixels that do not fit the typical statistics of the local neighborhood, i.e., outliers. Isolated noise pixels can therefore be removed with a median filter (Schowengerdt, 2007). The median filter is especially useful for removing shot noise (pixel values with no relation to the image scene) and has certain advantages such as it does not shift boundaries and has the minimal degradation to edges (Eliason and McEwen, 1990; Russ, 2002; Jensen, 2005). In this study, 3*3 neighborhood convolution mask (kernel) was applied to the PALSAR images. Image Add Back value was entered 60%. The Image Add Back value is the percentage of the original image that is included in the final output image. This part of the original image preserves the spatial context and is typically done to sharpen an image. The directional nature of geological lineaments accentuates the need for directional filtering to obtain maximum structural mapping efficacy. Edge enhancing filter highlights any changes of gradient within the image features such as structural lines (Carr, 1995; Sabins, 1996; Vincent, 1997; Tripathi and Gokhale, 2000; Research Systems, Inc., 2008).

In this study, for identifying linear features in particular directions and edge enhancement in the spatial domain, directional convolution filters were applied to the median resultant image. Directional filtering technique is a straightforward method for extracting edges in the spatial domain that approximates the first derivative between two adjacent pixels. The algorithm produces the first difference of the image input in the horizontal, vertical, and diagonal directions (Haralick et al., 1987; Carr, 1995; Sabins, 1996; Vincent, 1997; Jensen, 2005). As a result, many additional edges of diverse orientations are enhanced (Richards and Jia, 1999). The edges appear as a plastic shaded-relief format (embossing) in the image because of the 3-D impression conveyed by the filtering (Schowengerdt, 2007). Directional filter is used for producing artificial effects suggesting tectonically controlled linear features (Pour and Hashim, 2015a,b).

Directional filters were used to enhance specific linear trends in the median resultant image. Four principal directional filters: N-S, E-W, NE-SW, and NW-SE with 5*5 and 7*7 kernel sizes were applied to ScanSAR and Fine scenes, respectively. 5*5 kernel matrix was selected for ScanSAR scene to enhance rough/smooth and semi-rough features at regional scale in northern part of Peninsular Malaysia (Table 1). 7*7 kernel matrix was applied to Fine scenes for enhancing semi-smooth and smooth/rough features at district scale in the Kelantan state (Table 2) (Chavez and Bauer, 1982; Jensen, 2005). Directional filter angles were adjusted as N-S: 0°, E-W: 90°, NE-SW: 45°, and NW-SE: 135°. North (up) is zero degrees and the other angles are measured in the counterclockwise direction. Image Add Back value was entered 60%. Interpretation and analysis of geological features and enhanced lineaments was accomplished using systematic remote sensing techniques. Red-Green-Blue (RGB) colour-composite was used for different polarization configuration of PALSAR-2 data to provide visual interpretation of geological structures and lithological units in the study area. Image processing results were compared with the geological and general topography maps of Kelantan state (1:100,000 scale) (Department of Minerals and Geoscience Malaysia, 2003). Furthermore, for verification of the image processing results, fieldwork was conducted during a scientific expedition in Kelantan river basin between 20 and 25 June 2015, to collect data in landslide affected zones and flooded area by Global Positioning System (GPS) surveying, rock sampling and photographs recording. GPS survey was carried out using a Garmin® MONTERRA® with an average accuracy 5 m in 453 landslide affected location points in the study area.

Nat. Hazards Earth Syst. Sci. Discuss., doi:10.5194/nhess-2016-191, 2016
Manuscript under review for journal Nat. Hazards Earth Syst. Sci.
Published: 4 July 2016

5. Results and discussion

5.1 lineament extraction and lithology discrimination at regional scale

A wide-swath ScanSAR observation mode of PALSAR-2 was used for comprehensive analysis of major geological structures, which shows mega-geomorphology and mega-lineaments in the Kelantan state. Figure 3 shows RGB colour-composite of HH polarization channel in red, HV polarization channel in green and HH+HV polarization channel in blue for the ScanSAR median resultant image. The RGB colour-composite yields an image with great structural details and geomorphological information. The different colors in the image indicate different backscattering signals from the ground. The Main Range granites located in in the western part of the image and the Boundary Range granite in the east borders of Kelantan state appear as light green to green in colour, which shows the regions with high altitude in the scene (Fig. 3). Major transcrustal lineaments such the Bentong-Raub Suture Zone (BRSZ) and Lebir Fault Zone are also detected. Quarternary deposits, Triassic marine siliciclastics, volcaniclastics, sandstone and limestone are manifested as pink to purple tones consisting of lands with low elevation (Fig. 3). Lakes and main river systems are portrayed blue to dark blue in the image. In fact, the lines formed by blue to dark blue colour on the image are faults and fracture zones occupied by streams. The river pattern is one of the most important factors contributing to the lineament because it reflects the nature of the existing fracture system (Suzen and Toprak, 1998).

Figure 4 shows ScanSAR HV polarization image that is superimposed by general topography map of the Kelantan state (Department of Minerals and Geoscience Malaysia, 2003). It is evident that the morphology of the study area is largely controlled by rock type and structure. High elevation areas (500-100 m and <1000 m) in the Kelantan state are mountainous areas associated with Main Range granites (in the west) and Boundary Range granite (in the east),

Nat. Hazards Earth Syst. Sci. Discuss., doi:10.5194/nhess-2016-191, 2016
Manuscript under review for journal Nat. Hazards Earth Syst. Sci.
Published: 4 July 2016

which are detected as green to light green colour in the Figure 3. Hilly, plain and coastal areas with altitude between 500 to 50 m are associated with sedimentary rocks, which are manifested pink to purple colour in the Figure 3.

Figure 5 shows the resultant image map for N-S, NE-SW, and NW-SE (R: 0°, G: 45°, B: 135°) directional filters. Major change in deformation style is obvious from the west to the east in Figure 5. Structural analysis reveals four distinct parts from the west to the east, including (i) western part of the scene by ductile fabrics; (ii) western of the BRSZ affected mainly by brittle deformation; (iii) ductile-brittle deformation between the BRSZ and Lebir Fault Zone; and (iv) brittle-ductile fabrics between Lebir Fault Zone and eastern coastal line. Lineament occurrence in Figure 5 is mainly linked to the N-S trending of the BRSZ and Lebir Fault Zone. Generally, major faults are strike-slip with both dextral and sinistral movements, which trend N-S and NW-SE. NW-SE trending strike-slip faults moved sinistrally in the Lebir Fault Zone. The sinistral movement along the Lebir Fault Zone is responsible to the formation of folding and reverse faulting adjacent to the fault and surrounding area. These structures characterized transpressive tectonic regime in the Peninsular Malaysia (Richter et al., 1999; Harun, 2002).

The collision zone and compressional structures appear clearly in the west of the BRSZ in Main Range granites (Fig. 5). Deformation in this region shows the shortening zone oriented parallel to the BRSZ. Several faults, joints and fractures represent brittle deformation events in the region that mostly strike NW-SE. Generally, most of the short lineaments are clustered in the collision zone. Ductile deformation in the western margin of the image (Fig 5) includes upright asymmetrical mega folds with axial surfaces oriented W-E. Hence, the contractional strain direction affected this domain is from NE-SW followed by dextral shearing. The deformed area zone between the BRSZ and Lebir Fault Zone represents faults system and folded area. NW-SE striking strike-slip faults and NE-SW normal faults are dominated brittle structural elements within this domain. Ductile deformation is demonstrated by several open upright folds, which have W-E to NE-SW axial plans (Fig. 5). Brittle-ductile fabrics in the eastern part of image between Lebir Fault Zone and eastern coastal line illustrate curved shear zone that occupied by several N-S and NW-SE striking faults, fractures and joints. A mega concentric fold surrounds the shear zone with a WE striking axial surface. According to the orientation of the lineaments, sinistral movement along the Lebir Fault Zone is generated the tectonic features. Some N-S and NE-SW trending normal faults and small curvatures are also identifiable near the eastern coastal line (Fig. 5).

5.2 Lithology mapping at district scale

Figure 6 shows fine mode merged image of the northern and southern parts of the Kelantan state. In this figure, HH polarization channel was assigned to red colour, HV polarization channel to green colour and HH+HV polarization channels to blue colour for generating an RGB image for the study area. This colour combination produced an image map contains important information related to water bodies, wetlands and geological structural features. River systems and lakes appear black especially in north-eastern part of the image and wetlands as mauve colour (Fig. 6). Smooth surfaces such as calm water bodies appear dark in SAR images due to reflection of radar signal. Hence, no returning radar signal could be detected in receiving antenna (Thurmond et al., 2006; Pour and Hashim, 2015a). Besides, best soil moisture/wetness information is achievable from L-band microwave because it comes out from deeper soils. In fact, vegetation is almost transparent and roughness effects are negligible using L-band microwave for soil wetness mapping/monitoring (Jackson and Schmugge 1989; Lacava et al., 2005). Soil moisture is one the most important factors in hydro-geological hazards, especially since the soil response is affected by its status of saturation. Accordingly, the identification of wetlands is very important for flood forecasting and prevention in the state of Kelantan. Wetlands are more distributed in northern part of the study area (Fig. 6). A vast wetland (strong mauve colour) represents clearly in the central north segment of the image. Several wetlands as light to strong mauve colour are observable in central east, south and south-western part of the image (Fig. 6).

The RGB image map (Fig. 6) was compared with the geological map of the Kelantan state. It is evident that most of the detected wetlands are associated with sedimentary and metamorphic rocks. A few of the wetlands are located in the granites bedrock areas in the west (the Main Range granite) and east (the Boundary Range granite) of the state of Kelantan. The granites bedrock areas are all characterized by dissected hilly to mountainous terrain that gives rise to isolated highlands and mountain ranges (Fig. 6). These granitic areas represent the outcrops of a number of granite batholiths that are generally elongated along a N-S to NNW-SSE direction (Bignell and Snelling, 1977).

The amplitude of the radar signal is highly sensitive to the physical properties of the ground surface, which produces the brightness of the surface to vary much more than optical or infrared images (Robinson et al., 1999). Hence, combination of different polarization channels of fine mode PALSAR-2 data contains considerable information for rock discrimination. In this study, an RGB colour-composite was produced by assigning HV+HH polarization channels to red, HV/HH polarization channels to green and HV polarization channel to blue colour for detailed rock discrimination in the Kelantan state. Figure 7 represents the RGB merged image for the northern and southern parts of the Kelantan state. Granitic rocks are manifested as light green colour (strong green in high altitude area probably due to layover effect on SAR image (Gelautz et al., 1998; Franceschetti and Lanari, 1999)), while sedimentary and metamorphic rocks appears as a variety of tones such as brown, light brown, dark green, light blue and light red in the image (Fig. 7). In comparison

Nat. Hazards Earth Syst. Sci. Discuss., doi:10.5194/nhess-2016-191, 2016
Manuscript under review for journal Nat. Hazards Earth Syst. Sci.
Published: 4 July 2016

with geological map of the study area, it seems that brown and dark green hues are metamorphic rocks and light brown, light blue and light red colours are sedimentary rocks (clay, shale, conglomerate, sandstone and limestone). River systems and lakes are observable clearly as black meandering stream and water bodies especially in the northern segment of the region (Fig. 7).

5.3 Structural mapping at district scale and Landslide and flood risk delineation

Four directionally filtered images of fine mode observation, which contain enhanced information for set of lineaments in N-S, E-W, NE-SW and NW-SE direction, were used for lineament mapping in the Kelantan state. Figure 8 shows structural map for the Kelantan state, which is derived from the resultant image of directional filtering to HV polarization channel. It should be noted that the locations of wet lands are also portrayed in this figure. The most important structural features in the image map are fault zones, river systems and drainage lines patterns (Fig. 8). Within the study area two large fault zones are presented, which are the BRSZ in the north-west and Lebir Fault Zone in the south-east. The N-S, NE-SW and NNE-SSW lineament trends are commonly dominant in the image map. The dominant lineaments tend to run in the N-S direction, which is mainly linked to the N-S trending of the BRSZ (in the west) and Lebir Fault Zone (in the east). Additionally, few short NW-SE trending lineaments are detected in the western and eastern parts of the study area (Fig. 8). The N-S and NE-SW striking system distributed in the south eastern segment of the region is particularly related to Lebir Fault Zone. Pattern of the lineament map in north-western part of the image map displays the occurrence of BRSZ fault zone, which contains lineaments in N-S and NNE-SSW directions. Most of the short and smaller faults follow the N-S, NE-SW and NNE-SSW trends as the major fault systems in the Kelantan state. It seems

Nat. Hazards Earth Syst. Sci. Discuss., doi:10.5194/nhess-2016-191, 2016
Manuscript under review for journal Nat. Hazards Earth Syst. Sci.
Published: 4 July 2016

that the NW-SE faults are the youngest faults in the study area due to low frequency of lineaments in this trend. The major N-S trending faults are interpreted as oldest structures in Peninsular Malaysia and related to amalgamation of Gondwana-derived terranes during the Permian-Triassic, and NE-SW and NW-SE-trending faults are interpreted to be Late Triassic to Jurassic in age (Metcalfe, 2013b).

The occurrence and concentration of geological structural features in any region are related to rock type, thickness of uppermost weathered mantle and brittleness of rocks (Harris et al., 1960). In the Kelantan state, high concentrations of lineaments are associated with granitic rocks in higher terrains and low concentrations of lineaments are usually associated with lower terrains of metamorphic and sedimentary rocks. Tjia and Harun (1985) analyzed regional structures of Peninsular Malaysia and reported that many lineaments are very well displayed in areas underlain by granite, whereas in other areas they are poorly shown. Moreover, Akhir (2004) identified that high lineament concentrations in the Upper Perak Valley, Perak state, Peninsular Malaysia are closely related to higher terrain which is formed by more resistant rocks such as granite and sandstone, whereas low lineament concentrations are associated with lower terrain which is mainly formed by less resistant rock types such as shale and slate. As well, volcanic rocks in the Upper Perak Valley, Perak state encompass a low lineament concentration (Akhir, 2004).

The rivers in the study area are structurally controlled. They display zigzag patterns due to the presence of fractures, joints and faults with changes in orientation (Fig. 8). The drainage system in the Kelantan river basin shows dendritic, sub-dendritic and rectangular patterns (Fig. 8). It is evident that the drainage pattern is apparently being controlled by structure and lithology in the study area. However, several factors such as topography, soil type, bedrock type, climate and vegetation cover influence input, output and transport of sediment and water in a drainage system. The geological structures and lithologic variation have given a rise to different drainage patterns (Summerfield, 1991). For instance, dendritic and sub-dendritic pattern with a large number of tributaries are typical of drainage in areas of impermeable crystalline rock such as gneiss and/or sediment of uniform resistance (horizontal strata). The pattern is characteristic of essentially flat-lying and/or relatively homogeneous rocks and impervious soils with lack of structural control. Rectangular pattern is usually caused by jointing or faulting of the underlying bedrocks. It is usually associated with massive, intrusive igneous and metamorphic rocks (Summerfield, 1991). Therefore, it is assumed that the area with dendritic and sub-dendritic pattern is subjected to hydro-geological hazards such as flooding because of low infiltration runoff. Rectangular drainage pattern is susceptible zone that could be easily affected by landslide due to slope of the land, litho-structural conditions and speed of runoff. In the Kelantan river basin, most of the dendritic and sub-dendritic drainage patterns are detected in central part of the river basin (Fig. 8), which is consisted of sedimentary rocks. However, most of the rectangular drainage patterns are associated with igneous and metamorphic rocks in the western part of the Kelantan river basin (Fig. 8). Structural and topographical feature map of the Kelantan river basin is shown in Figure 9. It is evident that most of the dendritic and sub-dendritic drainage patterns are located in low lands and the rectangular drainage pattern is dominated in high lands in the Kelantan river basin.

5.4 Field observation

Field observations were conducted between 20 and 25 June 2015 to compare the detected high potential risk and susceptible zones with high damaged areas in recent flooding events in the Kelantan river basin. GPS surveying was carried out in Tanah Merah, Machang, Jeli, Kuala Krai and Gua Musang districts in the Kelantan river basin. 453 landslide affected zones and flooded areas locations were recorded in forest, rubber, bushes (degraded forest), mixed crops, oil palm, cleared land, urban area and agriculture lands. Rock samples were taken from the lithological units of landslide affected sites. Ground photographs were taken of the high damaged areas after 2015 flooding event. The analysis of field investigations data indicate that many of flooded areas were associated with high potential risk zones for hydro-geological hazards such as wetlands, urban areas, floodplain scroll, meander bend and dendritic and sub-dendritic drainage patterns. Most of the hydro-geological hazards zones are located in flat topography regions (Fig. 9). Flat topography with impervious soils/surface has low infiltration runoff, which yields more storm runoff during heavy monsoon rainfall compared to other regions. Figure 10 (A and B) shows meander bend and floodplain scroll zones in in the Kelantan river basin, which were flooded areas during 2015 flooding event.

Numerous landslides affected points were recorded in high-altitude segment of south and south-western part of the Kelantan state. As mentioned above, high drainage density of rectangular system is governed in this domain. The drainage density affects runoff, in that a high drainage density drains runoff water rapidly, decreases the lag-time and increases the peak of hydrograph. Consequently, the slope of the land in the south and south-western regions increases the speed and extent of water and sediment transportation to the Kelantan river basin during heavy monsoon rainfall. Most of the landslide affected points were located in topographic slope of metamorphic and quaternary rock units. However, some landslides occurred in fracture zones of weathered igneous rock units. Some large landslide affected zones were recorded in the intersection of longitude and latitude between (N 5° 08′ 02″, E 101° 58′ 53″), (N 5° 08′ 14″, E 101° 59′ 06″), (N 5° 08′ 24″, E 101° 59′ 21″) and (N 5° 09′ 03″, E 101° 59′ 41″). These landslide points were associated with N-S, NNE-SSW and NE-SW trending fault zones. Figure 11 (A and B) shows large landslide affected zones in south-western part of the Kelantan state.

6. Conclusions

Results of this investigation indicate that the PALSAR-2 onboard the ALOS-2 has proven to be successful advanced remote sensing satellite data for disasters monitoring in tropical environments. Analysis of the PALSAR-2 data provided significant information for identifying high potential risk and susceptible zones for natural hazards of geological origin in the Kelantan river basin, Malaysia. Wetlands, floodplain scroll, meander bend, dendritic and sub-dendritic drainage patterns and urban areas were identified as high potential risk zones for hydro-geological hazards. Landslide recurrence regions were detected in high-altitude segment of south and south-western part of the Kelantan state, which is dominated with high density of rectangular drainage pattern and topographic slope of metamorphic and quaternary rock units. Some of the large landslide zones were associated with N-S, NNE-SSW and NE-SW trending fault systems. Structural and topographical geology maps were produced for the Kelantan river basin that could be used to facilitate the planning of geo-hazards mitigation. In conclusion, the results of this investigation has great potential assistance in terms of total solution to flood disaster management in the Kelantan river basin by providing important source of information to assess the potential for many natural hazards of geological origin.

Acknowledgements

This study was conducted as a part of Transdisciplinary Research Grant Scheme (TRGS) (Vote no: R.J130000.7809.4L837), Ministry of Higher Education (MOHE), Malaysia. We are thankful to the Universiti Teknologi Malaysia for providing the facilities for this investigation.

Nat. Hazards Earth Syst. Sci. Discuss., doi:10.5194/nhess-2016-191, 2016
Manuscript under review for journal Nat. Hazards Earth Syst. Sci.
Published: 4 July 2016

References

Abdullah, A., Nassr, S., Ghaleeb. (2013). Remote sensing and geographic information system for fault segments mapping a study from Taiz area, Yemen. Journal of Geological Research, p.16.

Akhir, J.M., (2004). Lineament in enhanced remote sensing images: an example from the Upper Perak Valley, Perak Darul Ridwan. Geological Society of Malaysia, Bulletin, 48, 115-119.

Amri, K., Mahdjoub, Y., Guergour, L., (2011). Use of Landsat 7 ETM+ for lithological and structural mapping of Wadi Afara Heouine area (Tahifet–Central Hoggar, Algeria). Arabian Journal of Geosciences 4, 1273–1287.

Arikawa, Y., Osawa, Y., Hatooka, Y., Suzuki, S., Kankaku, Y. (2010). "Development Status of Japanese Advanced Land Observing Satellite-2," Proceedings of the SPIE Remote Sensing Conference, Toulouse, France, Vol. 7826, Sept. 20-23, 2010, 'Sensors, Systems, and Next-Generation Satellites XIV,' edited by Roland Meynart, Steven P. Neeck, Haruhisa Shimoda, doi: 10.1117/12.866675

Blau, P., (2014). "Japan's H-IIA Rocket successfully Launches ALOS-2 Radar Satellite," Spaceflight 101. May 24, 2014, URL: http://www.spaceflight101.com/h-iia-f24-launch-updates---alos-2.html

Bannert, D. (2000a). The application of remote sensing to natural hazard of geologic orgion-experience learned from GRAS-program of Unesco and IUGS. International Archives of Photogrammetry and Remote Sensing, Vol.XXXIII, PartB7, Amsterdam 2000.

Bannert, D. (2000b). Geological application of remote sensing (GARS), an IUGS/UNESCO joint program in the new millennium. Episodes 23(1), 37-39.

Bignell, J.D and Snelling, N.J. (1977). Geochronology of Malayan granites. Overseas Geology and Mineral Resources, I.G.S., London. 72 p.

Nat. Hazards Earth Syst. Sci. Discuss., doi:10.5194/nhess-2016-191, 2016
Manuscript under review for journal Nat. Hazards Earth Syst. Sci.
Published: 4 July 2016

Carr, J.R. (1995). Numerical analysis for the geological science. Prentice-Hall, Inc., pp:592.

Chavez, P.C. and Bauer, B. (1982). An automatic optimum kernel-size selection technique for edge enhancement. Remote Sensing of Environment 12, 23-38.

Clark, C.D. and Wilson, C., (1994). Spatial analysis of lineaments. Computers and Geosciences 20 (718), 1237-1258.

Dai, F.C., Lee. C.F. (2002). Landslide characteristics and slope instability modeling using GIS, Lantau Island, Hong Kong. Geomorphology, 42(3-4), 213-228.

Department of Minerals and Geoscience Malaysia (2003). Quarry Resource Planning for the State of Kelantan. Osborne and Chappel Sdn. Bhd.

Eagleman, J. R. and Lin, W.C. (1976). Remote Sensing of Soil Moisture by a 21-cm Passive Radiometer, J. Geophys. Res., 81, 3660-3666.

Eliason, E.M. and McEwen, A.S. (1990). Adaptive Box Filters for Removal of Random Noise from Digital Images. Photogrammetric Engineering & Remote Sensing, April, 1990, V56 No. 4, p. 453.

Earth Remote Sensing Data Analysis Center (ERSDAC) (2006). PALSAR user's guide. 1st Edition. March 2006.

Franceschetti, G., Lanari, R. Synthetic aperture radar processing. CRC Press, Boca Raton. 1999.

Ghani, A.A. (2009). Plutonism. In: Hutchison, C.S. and Tan, D.N.K., Eds., *Geology of Peninsular Malaysia*, Geological Society of Malaysia, Kuala Lumpur, 211-232.

Gelautz, M., Frick, H., Raggam, J., Burgstaller, J., Leberl., F. (1998). SAR image simulation and analysis of alpine terrain. ISPRS Journal of Photogrammetry & Remote Sensing, 53, 17-38.

Nat. Hazards Earth Syst. Sci. Discuss., doi:10.5194/nhess-2016-191, 2016
Manuscript under review for journal Nat. Hazards Earth Syst. Sci.
Published: 4 July 2016

Guzzetti, F., Carrara, A., Cardinali, M., Reichenbach, P. (1999). Landslide hazard evaluation: a review of current techniques and their application in multi-scale study, Central Italy. Geomorphology, 31(1-4), 181-216.

Harun, Z., (2002). Late Mesozoic-Early Tertiary faults of Peninsular Malaysia. Geological Society of Malaysia Annual Geological Conference. May 26-27, Kota Bharu, Kelantan, Malaysia.

Haralick, R.M., Sternberg, S.R., and Zhuang, X. (1987). Image Analysis Using Mathematical Morphology. IEEE Transactions on Pattern Analysis and Machine Intelligence, Vol. PAMI-9, No. 4, July 1987, pp. 532-550.

Harris, J.F., Tailor, G.L., Walper, J.L., (1960). Relation of deformational fractures in sedimentary rocks to regional and local structure. American Association of Petroleum Geologist Bulletin, 44, 1853-1873.

Hamimi, Z., El-Sawy, E.S.K., El-Fakharani, A., Matsah, M., Shujoon, A., El-Shafei, M.K., 2014. Neoproterozoic structural evolution of NE-trending Ad-Damm Shear Zone, Arabian Shield, Saudi Arabia. Journal of Asian Earth Sciences 99 (1), 51–63.

Hashim, M., Ahmad, S., Johari, M.A.M., Pour, A.B. (2013). Automatic lineament extraction in a heavily vegetated region using Landsat Enhanced Thematic Mapper (ETM+) imagery. Advances in Space Research 51, 874-890.

Henderson, F.M., Lewis, A.J. (1998). Principles and applications of imaging radar, manual of remote sensing. 3rd Edition. Vol.2.John Wiley and Sons, New York, 886 pp.

Heng, G.S., Hoe, T.G., Hassan, W.F.W. (2006). Gold mineralization and zonation in the state of Kelantan. Geological Scociety Malaysia Bulletin 52, 129-135.

Igarashi, T. (2001). ALOS Mission requirement and sensor specifications. Advances in Space Research 28(1), 127-131.

Nat. Hazards Earth Syst. Sci. Discuss., doi:10.5194/nhess-2016-191, 2016
Manuscript under review for journal Nat. Hazards Earth Syst. Sci.
Published: 4 July 2016

Jackson, T. J. and Schmugge, T.J. (1989). Passive Microwave Remote Sensing System for Soil Moisture: Some Supporting Research, IEEE Trans. Geosci. Rem. Sens., 27, 225-235, 1989.

Japan Aerospace Exploration Agency. (2014). ALOS-2/PALSAR-2 Level 1.1/1.5/2.1/3.1 GeoTIFF Product Format Description. http://www.eorc.jaxa.jp/ALOS-2/en/doc/format.htm.

Jensen, J.R. (2005). Introductory Digital Image Processing: A remote sensing perspective. Pearson Prentice Hall, Upper Saddle River NJ 07458. Third edition, p: 276-287.

Kankaku, Y., Osawa, Y., Hatooka Y., Suzuki, S. (2010). "Overview of Advanced Land Observing Satellite-2 (ALOS-2)" Proceedings of ISPRS Technical Commission VIII Symposium, Aug. 9-12, 2010, Kyoto, Japan.

Lacava, T., Greco, M., Leo, E. (2005). Monitoring soil wetness variations by means of satellite passive microwave observations: the hydroptimet study case. Natural Hazards and Earth System Sciences, 5, 583-592.

Lee, J.S., and Jurkevich, I. (1994). Speckle filtering of synthetic aperture radar images: a review. Remote Sensing Review. Vol: 8, pp:313-340.

Mardiana, S., Ahmad, A., Osman, K. (2000). Capability of RADARSAT data in monsoon flood monitoring. GIS Development, 1-6.

Metcalfe, I. (2000). The Bentong-Raub Suture Zone. Journal of Asian Earth Sciences. 18 , 691 – 712 .

Metcalfe, I. (2013a). Tectonic evolution of the Malay Peninsula. Journal of Asian Earth Sciences. 76, 195-213.

Metcalfe, I. (2013b). Gondwana dispersion and Asian accretion: Tectonic and palaeogeographic evolution of eastern Tethys. Journal of Asian Earth Sciences 66, 1-33.

Morelli, M., Piana, F. (2006). Comparison between remote sensed lineaments and geological structure in intensively cultivated hills (Monferrato and Langhe domains, NW Italy). International Journal of Remote Sensing 27(20), 4471–4493.

Nazaruddin, D.A., Fadilah, N.S.M., Zulkharnain, Z., Omar, S.A.S., Ibrahim, M.K.M. (2014). Geological Studies to Support the Tourism Site: A Case Study in the *Rafflesia* Trail, Near Kampung Jedip, Lojing Highlands, Kelantan, Malaysia. International journal of Geosciences, 835-851.

Pradhan, B. (2009). Flood susceptible mapping and risk area delineation using logistic regression, GIS and remote sensing. Journal of Hydrology 9, No: 2.

Pradhan, B., Shafiee, M., Pirasteh, S. (2009). Maximum flood prone area mapping using RADARSAT images and GIS: Kelantan river basin. International Journal of Geoinformatics, 5(2), 11-23.

Pradhan, B., Youssef, A.M. (2011). A100-yearmaximum flood susceptibility mapping using integrated hydrological and hydrodynamic models: Kelantan River Corridor, Malaysia. Journal of Flood Risk Management, 1-14.

Pour, B. A., Hashim, M, and van Genderen. J. (2013). Detection of hydrothermal alteration zones in a tropical region using satellite remote sensing data: Bau gold field, Sarawak, Malaysia. Ore Geology Reviews. 54, 181-196.

Pour, B. A., Hashim, M, Marghany. M (2014a). Exploration of gold mineralization in a tropical region using Earth Observing-1 (EO1) and JERS-1 SAR data: a case study from Bau gold field, Sarawak, Malaysia. Arabian Journal of Geosciences 7(6), 2393-2406.

Pour, B. A., Hashim, M. (2014b). Structural geology mapping using PALSAR data in the Bau gold mining district, Sarawak, Malaysia. Advances in Space Research, 54(4), 644-654.

Nat. Hazards Earth Syst. Sci. Discuss., doi:10.5194/nhess-2016-191, 2016
Manuscript under review for journal Nat. Hazards Earth Syst. Sci.
Published: 4 July 2016

Pour, A.B., Hashim, M., (2015a). Structural mapping using PALSAR data in the Central Gold Belt Peninsular Malaysia, Ore Geology Reviews 64, 13-22.

Pour, A.B., Hashim, M., (2015b). Integrating PALSAR and ASTER data for mineral deposits exploration in tropical environments: a case study from Central Belt, Peninsular Malaysia. International Journal of Image and Data Fusion 6(2), 170-188.

Raharimahefa, T., Kusky, T.M., 2007. Stuctural and remote sensing studies of the southern Betsimisaraka Suture, Madagascar. Gondwana Reseach 10, 186-197.

Raharimahefa, T., Kusky, T.M. 2009. Structural and remote sensing analysis of the Betsimisaraka Suture in northeastern Madagascar. Gondwana Reseach 15, 14-27.

Rahman, C.A. and Mohamed, K.R. (2001). Pemetaan Awalan Sumber Warisan Geologi Negeri Kelantan. In: Komoo, I., Tjia, H.D. and Leman, M.S., Eds., *Geological Heritage of Malaysia* (*Geoheritage Mapping and Geosite Characterization*), LESTARI UMK, Bangi.

Raj, J.K. (2009) Geomorphology. In: Hutchison, C.S. and Tan, D.N.K., Eds., *Geology of Peninsular Malaysia*, Geological Society of Malaysia, Kuala Lumpur, 5-29.

Ramli, M.F., Tripathi, N.K., Yusof, N., Shafri, H.Z.M., Rahman, Z.A., (2009). Lineament mapping in a tropical environment using Landsat imagery. International Journal of Remote Sensing 30 (23), 6277–6300.

Research Systems, Inc. (2008). *ENVI Tutorials*. Research Systems, Inc., Boulder, CO.

Richard, J.A., and Jia, X., (1999). Remote Sensing Digital Image Analysis, New York: Springer-Verlag, p: 363.

Richter, B., Schmidtke, E., Fuller, M., Harbury, N., Samsudin, A.R., (1999). Palaeomagnetism of Peninsular Malaysia. Journal of Asian Earth Sciences 17, 477–519.

Robinson, C., Kusky, T., El-Baz, F., and El-Etr, H., 1999. Using Radar Data to Assess Structural Controls from Variable Channel Morphology: Examples from the Eastern

Sahara: Proceeding of the Thirteen International Conference on Applied Geologic Remote Sensing, Vancouver, Canada, 1-3 March.

Rosenqvist, A., Shimada M., Chapman B. (2004). An overview of the JERS-1 SAR Global Boreal Forest Mapping (GBFM) project. Geoscience and Remote Sensing Symposium, IGARRS 0.4, Proceedings. 20-24 September 2004. Vol:2, p: 1033-1036.

Russ, J.C., (2002). The Image Processing Handbook, Boca Raton, FL: CRC Press, p:744.

Sabins, F.F. (1996). Remote sensing: Principal and Interpretation, (3rd Edn.), W.H. Freeman and Co.

Schwartz, M.O., Rajah, S.S., Askury, A.K., Putthapiban, P., Djaswadi, S., (1995). The Southeast Asian Tin Belt. Earth Science Reviews 38, 95-293.

Sheng, Y., and Xia, Z.G. (1996). A comprehensive evaluation of filters for radar speckle suppression. Geoscience and Remote Sensing Symposium, IGARSS.96, Remote sensing for sustainable future.vol: 3, p: 1559-1561.

Shimada, M., Isoguchi, O. (2002). JERS-1 SAR mosaics of South-EastAsia using calibrated path images. International Journal of Remote Sensing 23(7), 1507–1526.

Shimada, M. (2013). ALOS-2 science program. Proceedings of IGARSS (IEEE international Geoscience and Remote Sensing symposium), Melbourne, Australia, July 21-26, 2013.

Shimada, M., Watanabe, M., Motooka, T., Kankaku, Y., Suzuki, S. (2015). Calibration and validation of the PALSAR-2. Proceedings of the IGARSS (International Geoscience and Remote Sensing Symposium) 2015, Milan, Italy, July 26-31, 2015.

Schowengerdt, R.A., (2007). Remote sensing: models and methods for image processing. 3rd ed. Burlington, MA: Academic Press, Elsevier, p: 229–243.

Summerfield, M.A. (1991). Global Geomorphology. An Introduction to the Study of Landforms. Part IV, Chapter 16 (p.405-430). Harlow: Longman; New York: John Wiley Inc. ISBN 0 582 30156 4 (Longman), 0 470 21666 2 (Wiley).

Suzen, M.L., Toprak, V. (1998). Filtering of satellite images in geological lineament anlyses: an application to a fault zone in Central Turkey. International Journal of Remote Sensing 19(6), 1101–1114.

Suzen, M.L., Doyuran, V. (2004). Data driven bivariate landslide susceptibility assessment using geographical information systems: a method and application to Asarsuyu catchment, Turkey. Engineering Geology, 71(3-4), 303-321.

Suzuki, S., Kankaku Y., Imai, H., Osawa Y. (2012). "Overview of ALOS-2 and ALOS-3", Proceedings of SPIE,' Earth Observing Missions and Sensors: Development, Implementation, and Characterization II,' Vol. 8528, Kyoto, Japan, October 29, 2012, 852811 (November 9, 2012); doi:10.1117/12.979184

Suzuki, S. (2014). "Advanced Land Observing Satellite-2 "DAICHI-2" (ALOS-2) - Mission talk by team leaders," JAXA, May 2014, URL: http://global.jaxa.jp/projects/sat/alos2/leaders.html

Sveinsson, J.R., Benediktsson, J.A. (1996). Speckle reduction and enhancement of SAR image in the wavelet domain. Geoscience and Remote Sensing Symposium, IGARSS.96, Remote sensing for sustainable future.vol: 1, p: 63-66.

Tan, B. K., (1996). “Suture Zone” in peninsular Malaysia and Thailand: Implications for paleotectonic reconstruction of Southeast Asia. Journal of Southeast Asian Earth Sciences. 13, 243 – 249.

Tehrany, M.S., Pradhan, B., Jebur, M.N. (2013). Spatial prediction of flood susceptible areas using rule based decision tree (DT) and a novel ensemble bivariate and multivariate statistical models in GIS. Journal of Hydrology 504, 69–79.

Thurmond, A.K., Abdelsalam, M.G., Thurmond, J.B. (2006). Optical-radar-DEM remote sensing data integration for geological mapping in the Afar Depression, Ethiopia. Journal of African Earth Sciences 44, 119-134.

Tjia, H.D., Harun, Z. (1985). Regional structures of Peninsular Malaysia. Sains Malaysiana 14, 95-107.

Tjia, H.D., (1989). Major faults of Peninsular Malaysia on remotely sensed images. Sains Malaysiana 18(1), 101-114.

Tripathi, N.K. and Gokhale, V.G.K., (2000). Directional morphological image transforms for lineament extraction from remotely sensed images. International Journal of Remote Sensing 21(17), 3281–3292.

Unjah, T., Komoo, I. and Mohamad, H. (2001). Pengenalpastian Sumber Warisan Geologi di Negeri Kelantan. In: Komoo, I., Tjia, H.D. and Leman, M.S., Eds., *Geological Heritage of Malaysia* (*Geoheritage Mapping and Geosite Characterization*), LESTARI UMK, Bangi.

van der Pluijm, B.A., Marshak, S., 1997. Earth Structure - An Introduction to Structural Geology and Tectonics. WCB-McGraw-Hill.

Vincent, R.K., 1997. Fundamentals of Geological and Environmental Remote Sensing, Prentice Hall, New Jersey, pp: 366.

Woodhouse, I.H. (2006). Introduction to microwave remote sensing. CRC Press, Taylor & Francis Group, Boca Raton.

Yamamoto, T., Kawano, I., Iwata, T., Arikawa, Y., Itoh, H., Yamamoto, M., Nakajima, K. (2013). Autonomous Precision Orbit Control of ALOS-2 for Repeat-Pass SAR Interferometry. Proceedings of IGARSS (IEEE International Geoscience and Remote Sensing Symposium), Melbourne, Australia, July 21-26, 2013.

Nat. Hazards Earth Syst. Sci. Discuss., doi:10.5194/nhess-2016-191, 2016
Manuscript under review for journal Nat. Hazards Earth Syst. Sci.
Published: 4 July 2016

Natural Hazards and Earth System Sciences
Open Access
Discussions

Figure captions

Figure 1. Location of the Kelantan state in Peninsular Malaysia.

Figure 2. Geologic map of the Kelantan state (modified from Department of Minerals and Geoscience Malaysia, 2003).

Figure 3. RGB colour combination (HH, HV and HH+HV polarization channels) of PALSAR-2 Scan SAR scene covering northern part of the Peninsular Malaysia. Black rectangle shows covering area by fine mode merged images of the northern and southern parts of the Kelantan state in this study.

Figure 4. ScanSAR HV polarization image of the Kelantan state superimposed by general topography map.

Figure 5. ScanSAR image map derived from N-S (0°), NE-SW (45°), and NW-SE (135°) directional filters for northern part of the Peninsular Malaysia. Explanation for the figure: dashed black lines = major faults; dot-dashed lines = folds and curvilinear; red lines = faults and fractures.

Figure 6. RGB colour-composite image of HH, HV and HH+HV polarization channels derived from fine mode merged image of the northern and southern parts of the Kelantan state.

Figure 7. RGB colour-composite image of HV+HH, HV/HH and HV polarization channels derived from fine mode merged image of the northern and southern parts of the Kelantan state.

Figure 8. Structural lineament map of the Kelantan state derived from directional filtering to HV polarization channel.

Figure 9. Structural and topographical feature map of the Kelantan river basin.

Figure 10. (A): Meander bend; and (B): floodplain scroll zone in the Kelantan river basin.

Figure 11. Large landslide affected zones (A and B) in south-western part of the Kelantan state.

Table captions

Table 1: Directional filters with 5*5 kernel matrix.

Table 2: Directional filters with 7*7 kernel matrix.

Nat. Hazards Earth Syst. Sci. Discuss., doi:10.5194/nhess-2016-191, 2016
Manuscript under review for journal Nat. Hazards Earth Syst. Sci.
Published: 4 July 2016

Natural Hazards and Earth System Sciences
Open Access
Discussions

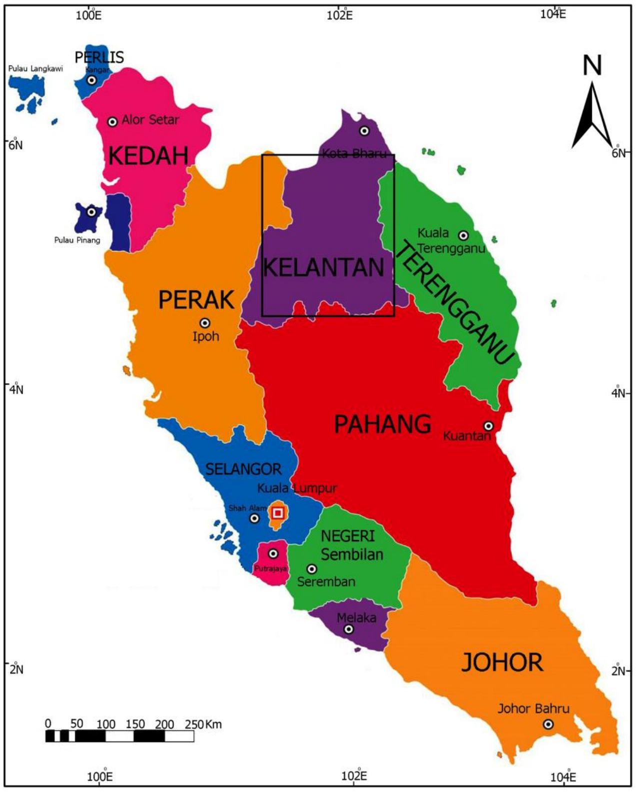

Figure 1. Location of the Kelantan state in Peninsular Malaysia.

Nat. Hazards Earth Syst. Sci. Discuss., doi:10.5194/nhess-2016-191, 2016
Manuscript under review for journal Nat. Hazards Earth Syst. Sci.
Published: 4 July 2016

Natural Hazards and Earth System Sciences
Open Access
Discussions

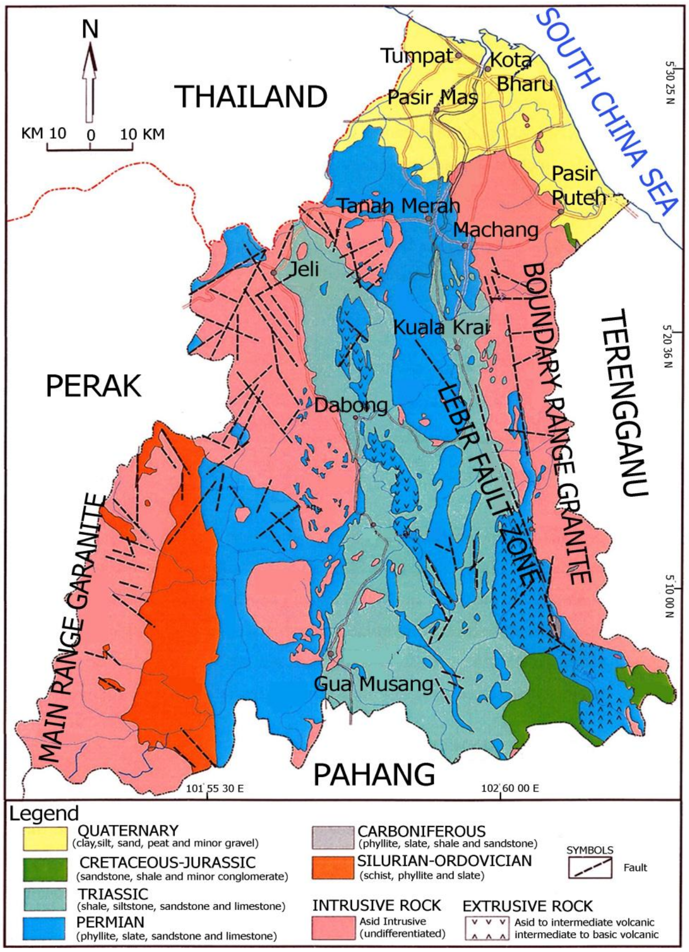

Figure 2. Geologic map of the Kelantan state (modified from Department of Minerals and Geoscience Malaysia, 2003).

Nat. Hazards Earth Syst. Sci. Discuss., doi:10.5194/nhess-2016-191, 2016
Manuscript under review for journal Nat. Hazards Earth Syst. Sci.
Published: 4 July 2016

821

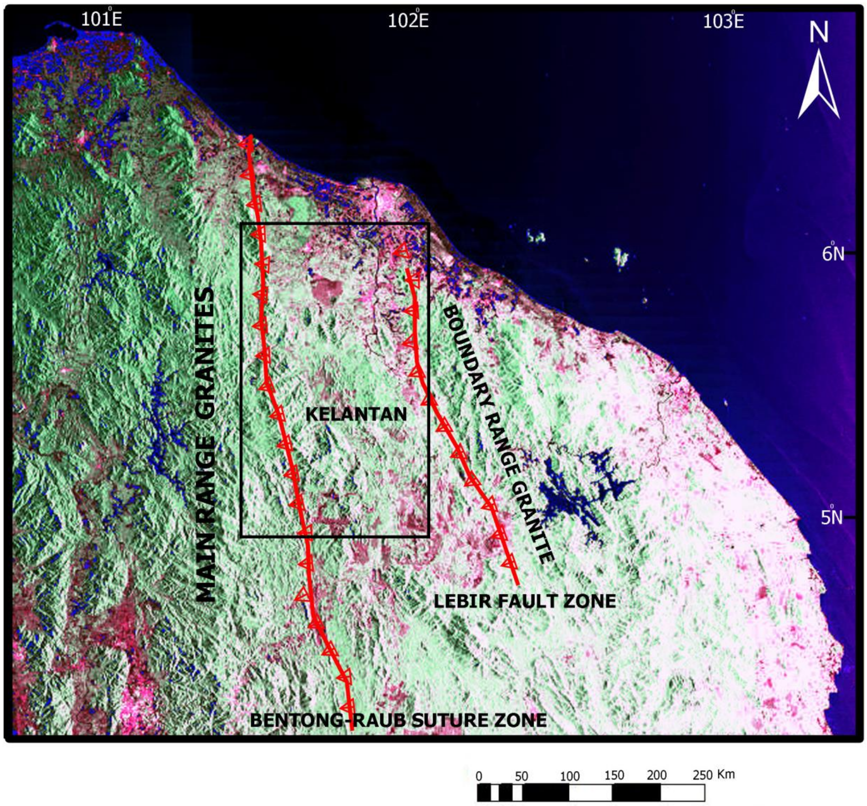

822
823
824
825 Figure 3. RGB colour combination (HH, HV and HH+HV polarization channels) of
826 PALSAR-2 Scan SAR scene covering northern part of the Peninsular Malaysia. Black
827 rectangle shows covering area by fine mode merged images of the northern and southern
828 parts of the Kelantan state in this study.

829

830

831

832

833

834

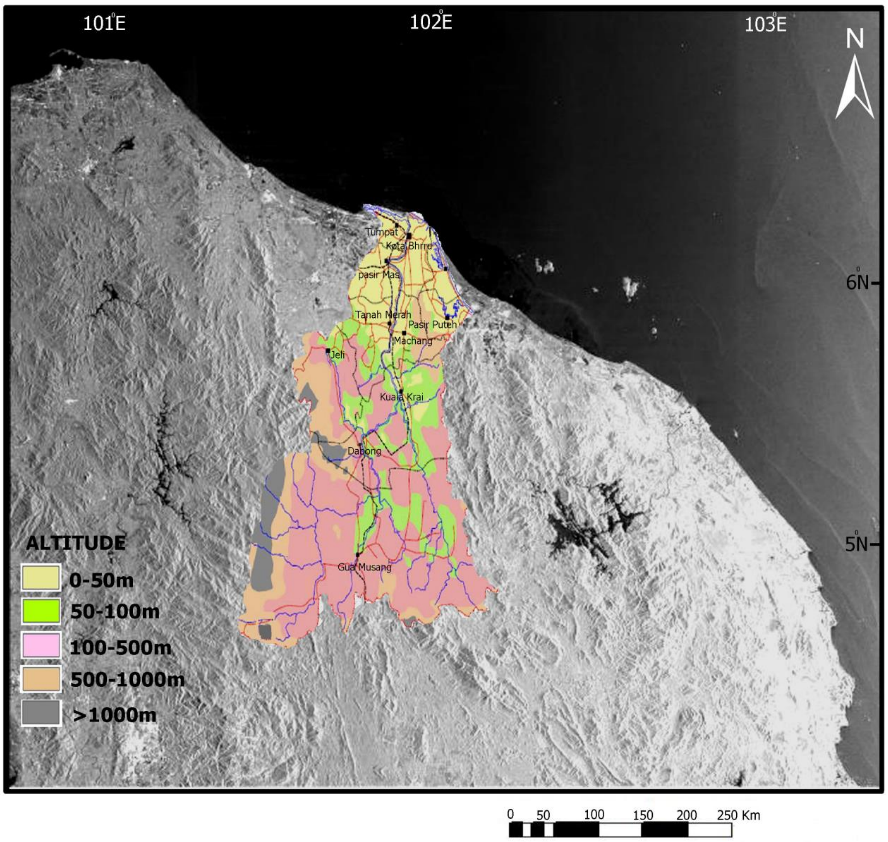

Figure 4. ScanSAR HV polarization image of the Kelantan state superimposed by general topography map.

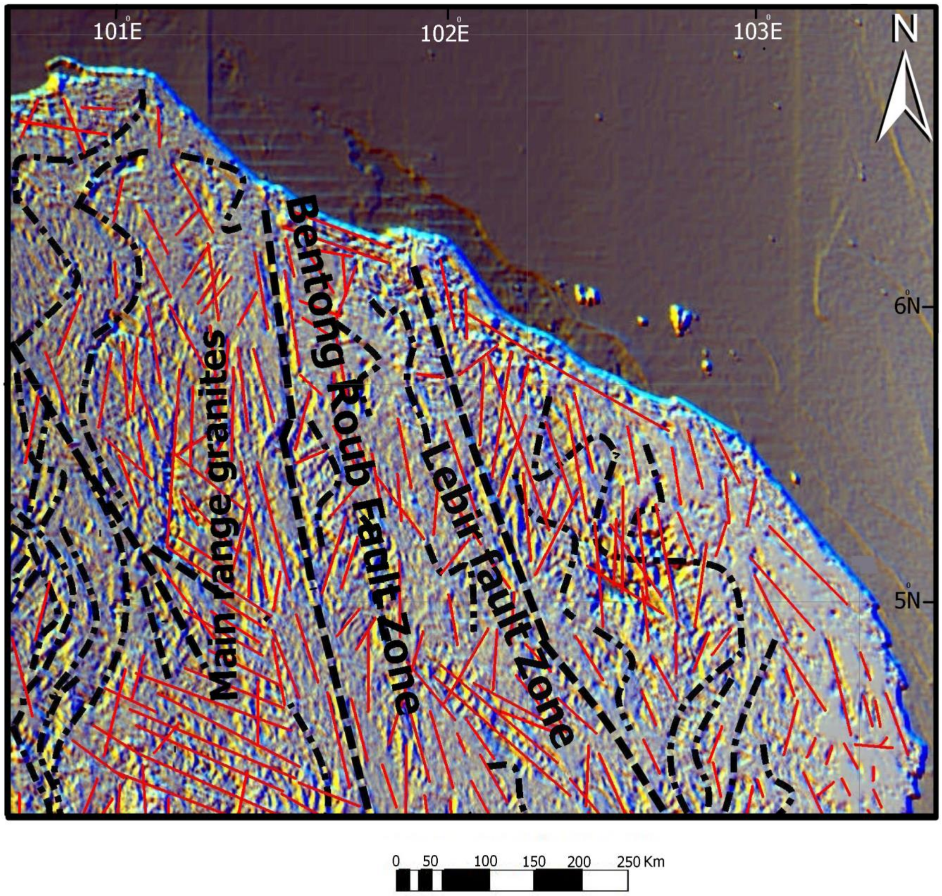

Figure 5. ScanSAR image map derived from N-S (0°), NE-SW (45°), and NW-SE (135°) directional filters for northern part of the Peninsular Malaysia. Explanation for the figure: dashed black lines = major faults; dot-dashed lines = folds and curvilinear; red lines = faults and fractures.

Nat. Hazards Earth Syst. Sci. Discuss., doi:10.5194/nhess-2016-191, 2016
Manuscript under review for journal Nat. Hazards Earth Syst. Sci.
Published: 4 July 2016

Natural Hazards and Earth System Sciences
Open Access
Discussions

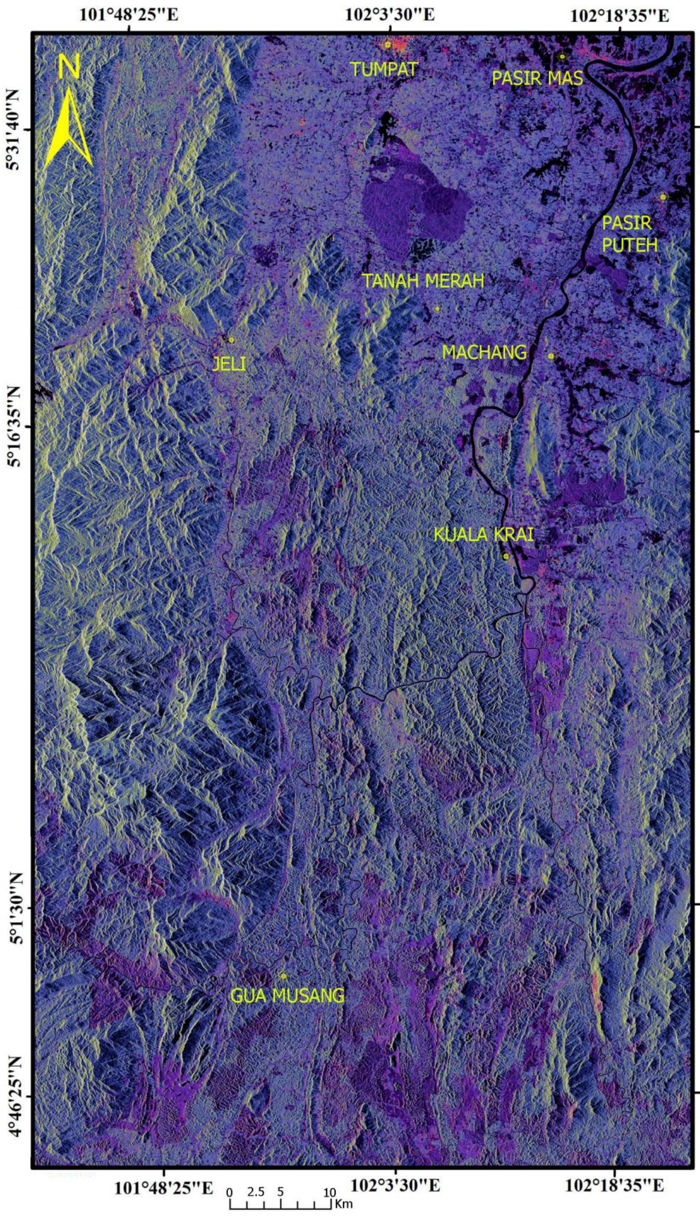

855

856

857 Figure 6. RGB colour-composite image of HH, HV and HH+HV polarization channels
858 derived from fine mode merged image of the northern and southern parts of the Kelantan
859 state.

Nat. Hazards Earth Syst. Sci. Discuss., doi:10.5194/nhess-2016-191, 2016
Manuscript under review for journal Nat. Hazards Earth Syst. Sci.
Published: 4 July 2016

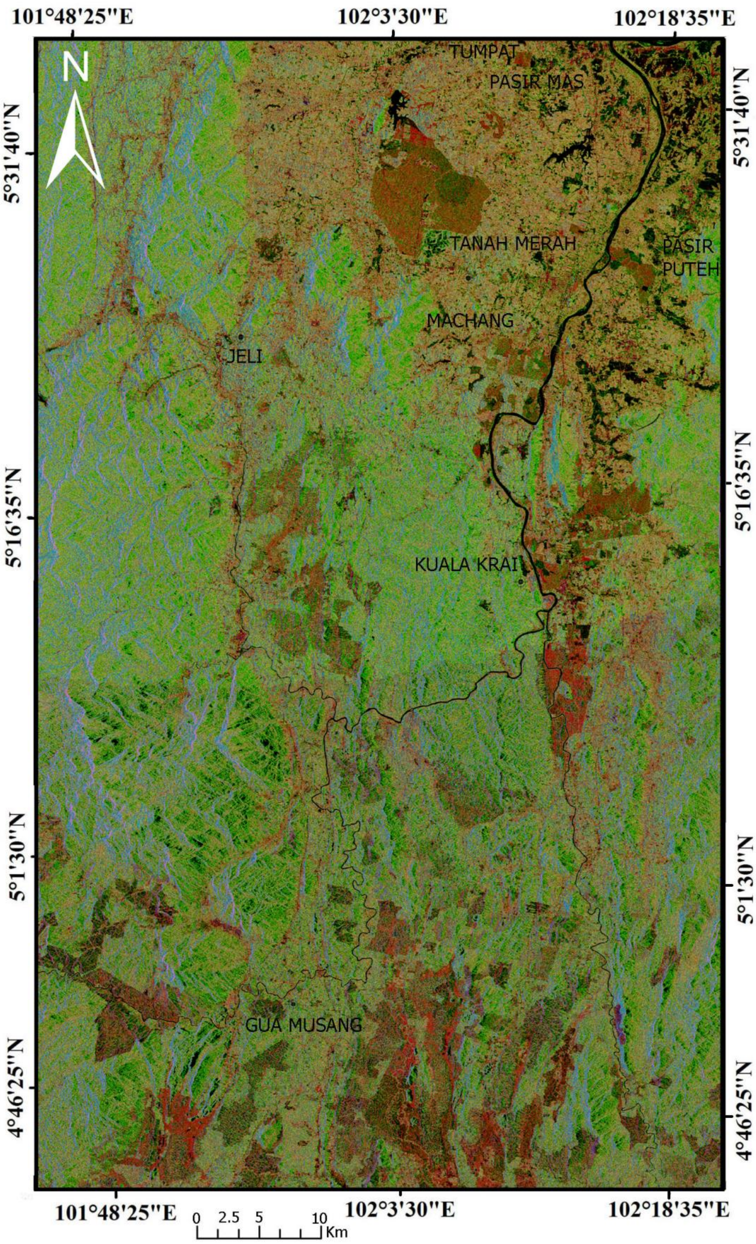

Figure 7. RGB colour-composite image of HV+HH, HV/HH and HV polarization channels derived from fine mode merged image of the northern and southern parts of the Kelantan state.

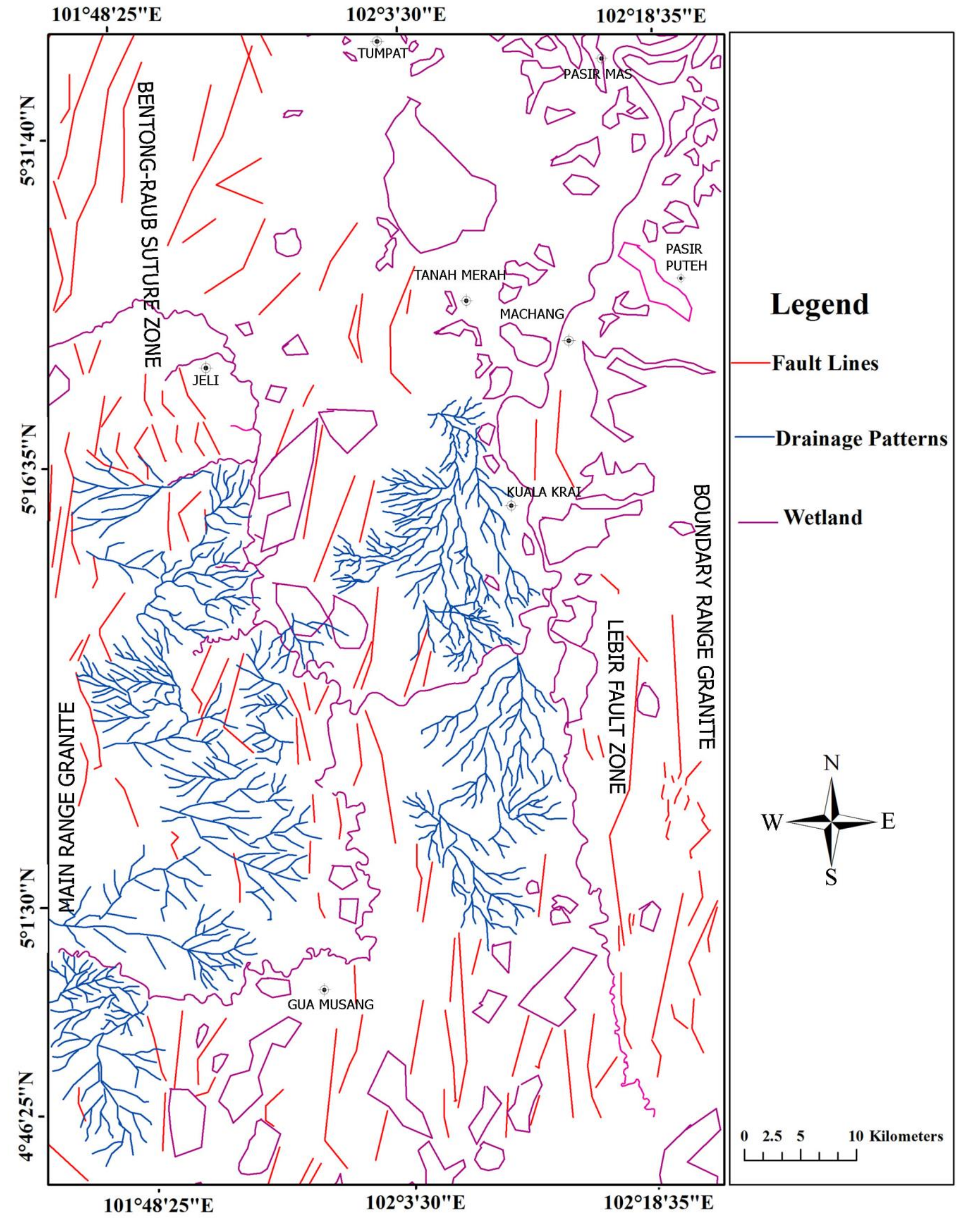

Figure 8. Structural lineament map of the Kelantan state derived from directional filtering to HV polarization channel.

Nat. Hazards Earth Syst. Sci. Discuss., doi:10.5194/nhess-2016-191, 2016
Manuscript under review for journal Nat. Hazards Earth Syst. Sci.
Published: 4 July 2016

Natural Hazards and Earth System Sciences
Open Access
Discussions

872

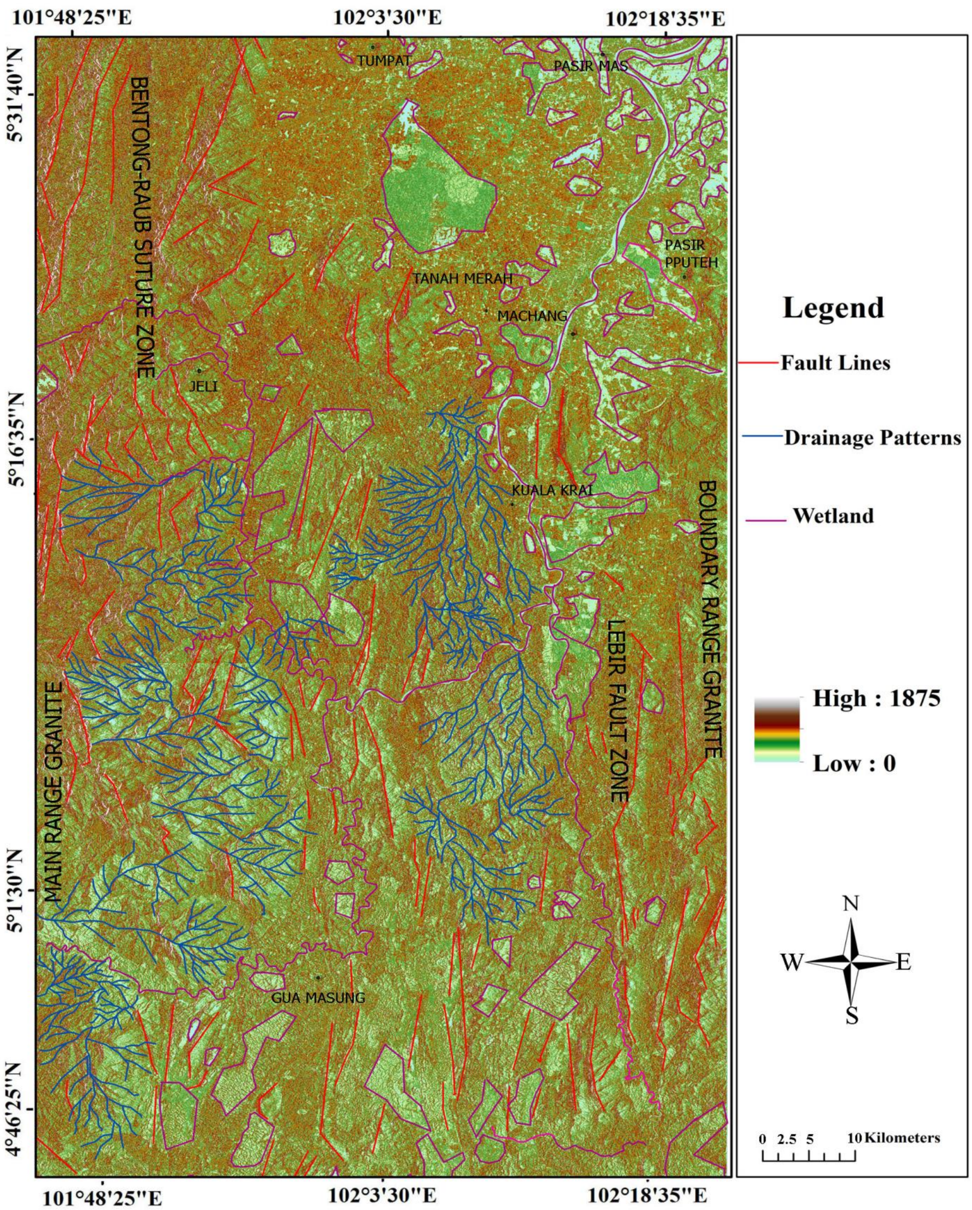

873

874 Figure 9. Structural and topographical feature map of the Kelantan river basin.

875

876

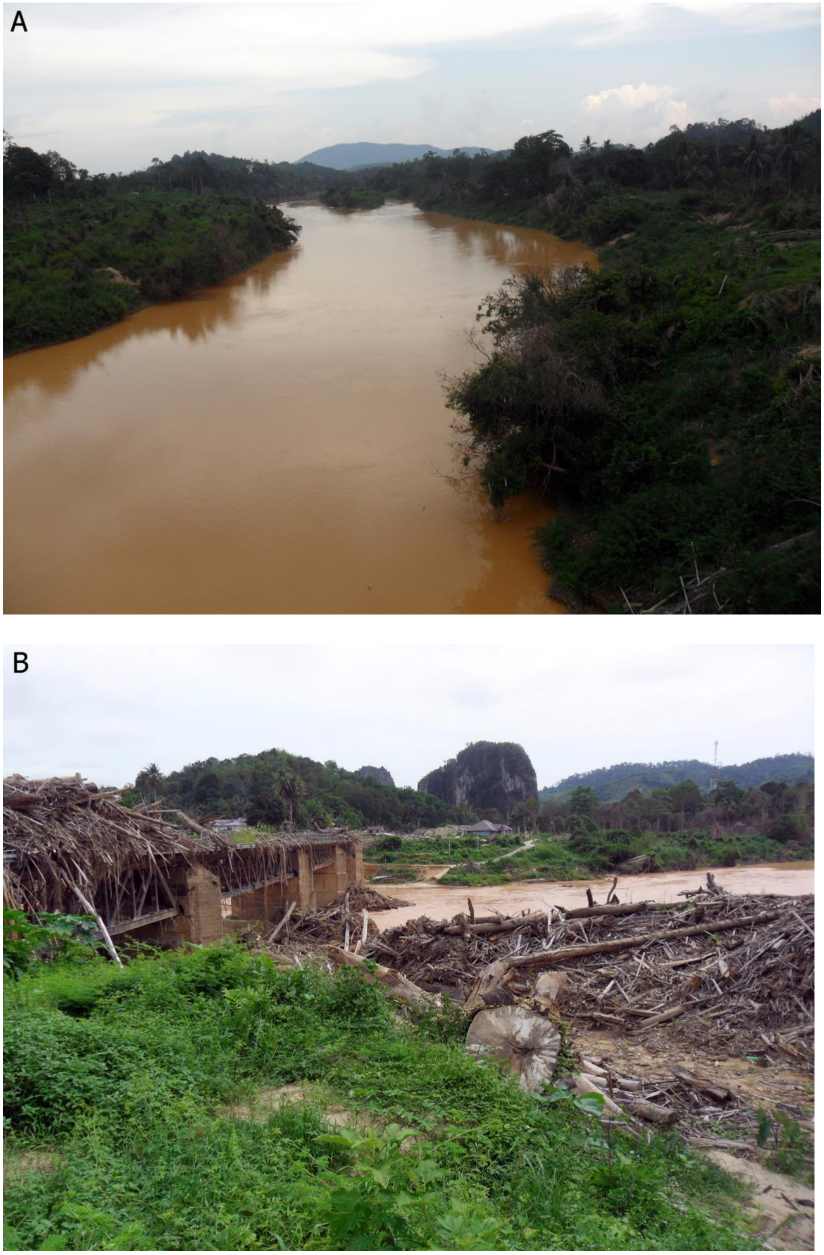

Figure 10. (A): Meander bend; and (B): floodplain scroll zone in the Kelantan river basin.

Nat. Hazards Earth Syst. Sci. Discuss., doi:10.5194/nhess-2016-191, 2016
Manuscript under review for journal Nat. Hazards Earth Syst. Sci.
Published: 4 July 2016

Natural Hazards and Earth System Sciences
Open Access
Discussions

Figure 11. Large landslide affected zones (A and B) in south-western part of the Kelantan state.

Nat. Hazards Earth Syst. Sci. Discuss., doi:10.5194/nhess-2016-191, 2016
Manuscript under review for journal Nat. Hazards Earth Syst. Sci.
Published: 4 July 2016

Table 1: Directional filters with 5*5 kernel matrix.

N-S				
-1.0000	-1.0000	0.0000	1.0000	1.0000
-1.0000	-1.0000	0.0000	1.0000	1.0000
-1.0000	-1.0000	0.0000	1.0000	1.0000
-1.0000	-1.0000	0.0000	1.0000	1.0000
-1.0000	-1.0000	0.0000	1.0000	1.0000
-1.0000	-1.0000	0.0000	1.0000	1.0000
-1.0000	-1.0000	0.0000	1.0000	1.0000
E-W				
-1.0000	-1.0000	-1.0000	-1.0000	-1.0000
-1.0000	-1.0000	-1.0000	-1.0000	-1.0000
0.0000	0.0000	0.0000	-0.0000	-0.0000
1.0000	1.0000	1.0000	1.0000	1.0000
1.0000	1.0000	1.0000	1.0000	1.0000
NE-SW				
-1.4142	-1.4142	-0.7071	0.0000	0.0000
-1.4142	-1.4142	-0.7071	0.0000	0.0000
-0.7071	-0.7071	0.0000	0.7071	0.7071
0.0000	0.0000	0.7071	1.4142	1.4142
0.0000	0.0000	0.7071	1.4142	1.4142
NW-SE				
0.0000	0.0000	-0.7071	-1.4142	-1.4142
0.0000	0.0000	-0.7071	-1.4142	-1.4142
0.7071	0.7071	0.0000	-0.7071	-0.7071
1.4142	1.4142	0.7071	0.0000	0.0000
1.4142	1.4142	0.7071	0.0000	0.0000

Nat. Hazards Earth Syst. Sci. Discuss., doi:10.5194/nhess-2016-191, 2016
Manuscript under review for journal Nat. Hazards Earth Syst. Sci.
Published: 4 July 2016

Natural Hazards and Earth System Sciences
Open Access
EGU
Discussions

Table 2: Directional filters with 7*7 kernel matrix.

N-S						
-1.0000	-1.0000	-1.0000	0.0000	1.0000	1.0000	1.0000
-1.0000	-1.0000	-1.0000	0.0000	1.0000	1.0000	1.0000
-1.0000	-1.0000	-1.0000	0.0000	1.0000	1.0000	1.0000
-1.0000	-1.0000	-1.0000	0.0000	1.0000	1.0000	1.0000
-1.0000	-1.0000	-1.0000	0.0000	1.0000	1.0000	1.0000
-1.0000	-1.0000	-1.0000	0.0000	1.0000	1.0000	1.0000
-1.0000	-1.0000	-1.0000	0.0000	1.0000	1.0000	1.0000
E-W						
-1.0000	-1.0000	-1.0000	-1.0000	-1.0000	-1.0000	-1.0000
-1.0000	-1.0000	-1.0000	-1.0000	-1.0000	-1.0000	-1.0000
-1.0000	-1.0000	-1.0000	-1.0000	-1.0000	-1.0000	-1.0000
0.0000	0.0000	0.0000	-0.0000	-0.0000	-0.0000	-0.0000
1.0000	1.0000	1.0000	1.0000	1.0000	1.0000	1.0000
1.0000	1.0000	1.0000	1.0000	1.0000	1.0000	1.0000
1.0000	1.0000	1.0000	1.0000	1.0000	1.0000	1.0000
NE-SW						
-1.4142	-1.4142	-1.4142	-0.7071	0.0000	0.0000	0.0000
-1.4142	-1.4142	-1.4142	-0.7071	0.0000	0.0000	0.0000
-1.4142	-1.4142	-1.4142	-0.7071	0.0000	0.0000	0.0000
-0.7071	-0.7071	-0.7071	0.0000	0.7071	0.7071	0.7071
0.0000	0.0000	0.0000	0.7071	1.4142	1.4142	1.4142
0.0000	0.0000	0.0000	0.7071	1.4142	1.4142	1.4142
0.0000	0.0000	0.0000	0.7071	1.4142	1.4142	1.4142
NW-SE						
0.0000	0.0000	0.0000	-0.7071	-1.4142	-1.4142	-1.4142
0.0000	0.0000	0.0000	-0.7071	-1.4142	-1.4142	- 1.4142
0.0000	0.0000	0.0000	-0.7071	-1.4142	-1.4142	-1.4142
0.7071	0.7071	0.7071	0.0000	-0.7071	-0.7071	-0.7071
1.4142	1.4142	1.4142	0.7071	0.0000	0.0000	0.0000
1.4142	1.4142	1.4142	0.7071	0.0000	0.0000	0.0000
1.4142	1.4142	1.4142	0.7071	0.0000	0.0000	0.0000